THE JOURNAL OF PHYSICAL CHEMISTRY A

Article

pubs.acs.org/JPCA

Highly Emissive Whole Rainbow Fluorophores Consisting of 1,4-Bis(2-phenylethynyl)benzene Core Skeleton: Design, Synthesis, and Light-Emitting Characteristics

Yoshihiro Yamaguchi,* Takanori Ochi, Yoshio Matsubara, and Zen-ichi Yoshida*

Department of Chemistry, Faculty of Science and Engineering, Kinki University, 3-4-1 Kowakae, Higashi-Osaka, Osaka 577-8502, Japan

Supporting Information

ABSTRACT: To create the whole-rainbow-fluorophores (WRF) having the small $\Delta\lambda_{em}$ (the difference of λ_{em} between a given fluorophore and nearest neighboring fluorophore having the same core skeleton) values (<20 nm) in full visible region (λ_{em}: 400−650 nm), the high log ε (>4.5), and the high Φ_f (>0.6), we investigated molecular design, synthesis, and light-emitting characteristics of the π-conjugated molecules (D/A-BPBs) consisting of 1,4-bis(phenylethynyl)benzene (BPB) modified by donor groups (OMe, SMe, NMe_2, and NPh_2) and an acceptor group (CN). As a result, synthesized 20 D/A-BPBs (**1a−5d**) were found to be the desired WRF. To get the intense red fluorophore (Φ_f > 0.7, λ_{em} > 610 nm), we synthesized new compounds (**5e−5i**) and elucidated their photophysical properties in $CHCl_3$ solution. As a result, **5h**, in which a 4-cyanophenyl group is introduced to the *para*-position of two benzene rings in the terminal NPh_2 group of **5d**, was found to be the desired intense red fluorophore (log ε = 4.56, Φ_f = 0.76, λ_{em} = 611 nm). The intramolecular charge-transfer nature of the S_1 state of WRF (**1a−5d**) was elucidated by the positive linear relationship between optical transition energy (ν_{em}) from the S_1 state to the S_0 state and HOMO(D)−LUMO(A) difference, and the molecular orbitals calculated with the DFT method. It is demonstrated that our concept ($\Phi_f = 1/(\exp(-A_\pi) + 1)$) connected with the relationship between Φ_f and magnitude (A_π) of π conjugation length in the S_1 state can be applied to WRF (**1a−5d**). It is suggested that the prediction of Φ_f from a structural model can be achieved by the equation $\Phi_f = 1/(\exp(-((\tilde{\nu}_a - \tilde{\nu}_f)^{1/2} \times a^{3/2}) + 1)$, where $\tilde{\nu}_a$ and $\tilde{\nu}_f$ are the wavenumber (cm^{-1}) of absorption and fluorescence peaks, respectively, and a is the calculated molecular radius. From the viewpoint of application of WRF to various functional materials, the light-emitting characteristics of **1a−5i** in doped polymer films were examined. It was demonstrated that **1a−5i** dispersed in two kinds of polymer film (PST and PMMA) emit light at the whole visible region and have the small $\Delta\lambda_{em}$ values (<20 nm) and the high Φ_f values (>0.6). Therefore, the present D/A-BPBs can be said to be the desired WRF even in the doped polymer film.

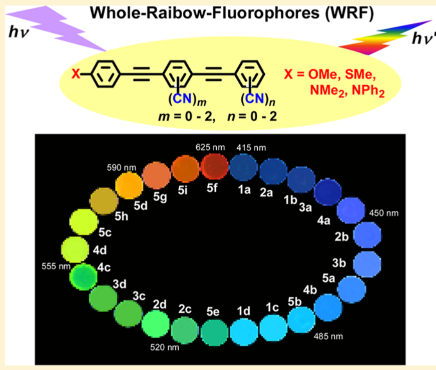

■ INTRODUCTION

Highly emissive fluorophores are utilized extensively not only as biosensors and biolabeling-agents in life science[1−7] but also as optoelectronic devices in materials science such as organic light-emitting diodes (OLEDs),[8−13] organic field-effect transistors (OFETs),[14−17] and organic solar cells.[18−24] Judging from such circumstances, it should be of particular importance to discover new fluorescent materials that have emission wavelengths adaptable for various applications mentioned above. Thus, the creation of highly emissive π-conjugated systems (fluorophores) consisted of the same skeleton whose fluorescence covers the full visible region is an attractive subject. Especially, the achievement of emission in full visible region employing the shortest π-conjugated systems without changing the core skeleton should be an intriguing theme to be challenged.

For creation of the ideal fluorophores, the emission in the full visible region, the high molar absorption coefficient (log ε) and quantum yield (Φ_f) are required. Although several papers have been reported for the creation of full-color-fluorophores (FCF, Figure 1) such as oligo(p-phenylenevinylene)s (OPV),[25,26] cross-conjugated bis-enediynes,[27] boron-containing π-conjugated systems,[28−31] silafluorenes,[32] 1,2-dihydropyrrolo[3,4-b]-indolizin-3-one,[33−36] organometallic complexes,[37−42] and other π-conjugated systems,[43−47] there have been remained the following problems to be solved, (1) low log ε and Φ_f, (2) two or more emission bands, and (3) large $\Delta\lambda_{em}$ values ($\Delta\lambda_{em}$ > 30−40 nm). The $\Delta\lambda_{em}$ is defined as the difference of emission maximum wavelength (λ_{em}) between a given fluorophore and another fluorophore whose λ_{em} is close to the former (nearest neighboring fluorophore). The increase in $\Delta\lambda_{em}$ values was found to be remarkable at the longer wavelength region than 550 nm (green) in FCF systems.

We have challenged to create the whole-rainbow-fluorophores (WRF, Figure 1) having the small $\Delta\lambda_{em}$ values (<20 nm) in the

Received: May 28, 2015
Revised: July 17, 2015

DOI: 10.1021/acs.jpca.5b05077
J. Phys. Chem. A XXXX, XXX, XXX−XXX

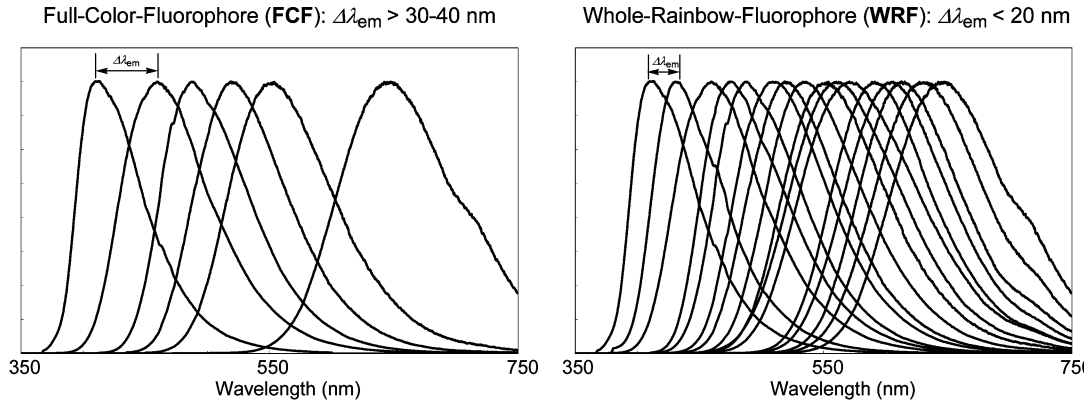

Figure 1. Features of fluorescence spectra for full-color-fluorophores (FCF) and whole-rainbow-fluorophores (WRF).

full visible region (λ_{em}: 400–650 nm), the high log ε (>4.5), and the high Φ_f (>0.6). Of those, the small $\Delta\lambda_{em}$ value is particularly important and useful for the application in various fields because of the possibility of the wide selectivity of color and control of delicate color.

We have chosen oligo(*p*-phenyleneethnylene)s (OPE)[48−59] hydrocarbons as the π-conjugated core skeleton because of the flexibility in their synthetic strategies, though the system seems to have a disadvantage for the creation of fluorophore compared with OPV[60−73] hydrocarbons as shown in Figure 2, assuming

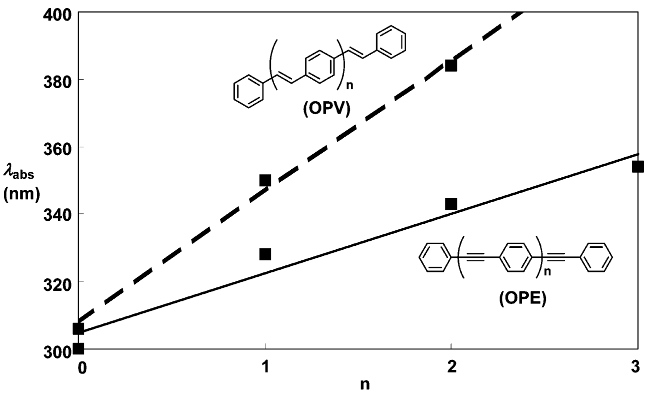

Figure 2. Relationship of absorption maximum (λ_{abs}) with π conjugation length (n) in OPE and OPV systems.

that the Stokes shifts of OPV and OPE are almost close to each other. After some synthetic trials, we succeeded in the creation of the desired WRF using OPE as the π-conjugated core skeleton, which is described herein.

■ RESULTS AND DISCUSSION

Molecular Design for WRF. On the basis of the preliminary experiments, we have chosen 1, 4-bis(phenylethynyl)benzene (BPB) as the most desirable π-conjugated core skeleton for creation of fluorophores described here. Although BPB itself fluoresces in ultraviolet region, the dramatic bathochromic shift of λ_{em} (visual emission) and the increase in Φ_f and log ε values are observed by introduction of donor/acceptor groups (as shown in Figure 3), suggesting that the donor/acceptor tuning should be effective method for the creation of highly emissive fluorophores.[74−85]

Furthermore, it has been found that donor/acceptor modification shown in structure **A** is superior to that shown in structure **B** for emission in the visible region (Figure 4).[86,87]

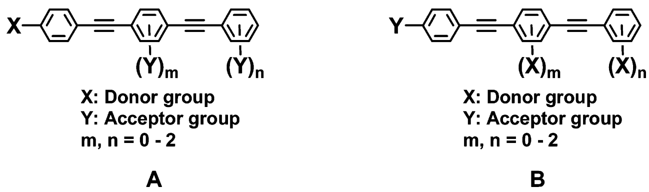

Figure 4. Tuning mode of BPB by donor/acceptor group.

On the basis of these results (the effectiveness of donor/acceptor tuning, Figure 3) and the superiority of tuning mode A (see Figure 4), 20 compounds (D/A-BPBs: Type I, Type II, Type III, Type IV, and Type V) were designed as shown in Figure 5.

In the previous paper[88] we reported that the optical transition energy (ν_{em}: cm^{-1}) from the excited singlet (S_1) state to the ground (S_0) state correlates linearly with the difference between the HOMO of the donor blocks (HOMO(D)) and the LUMO of the acceptor blocks (LUMO(A)) (abbreviated as HOMO(D)−LUMO(A) difference) in the D/A-OPE system. Therefore, the positive linear relationship between ν_{em} and the HOMO(D)−LUMO(A) difference is considered to be useful for the prediction of λ_{em} in D/A-OPE systems. The HOMO(D) values, LUMO(A) values, HOMO(D)−LUMO(A) difference values, and predictable λ_{em} values calculated by the DFT method for the designed 20 D/A-BPBs are summarized in Figure 6. As

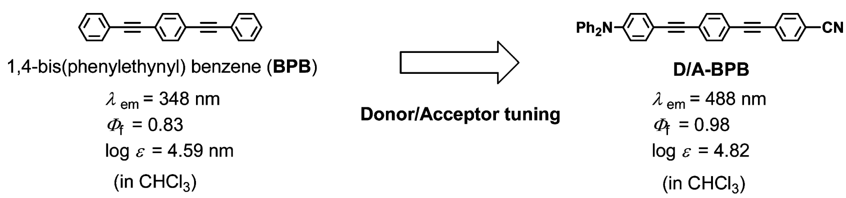

Figure 3. Effect of donor/acceptor tuning in BPB.

DOI: 10.1021/acs.jpca.5b05077
J. Phys. Chem. A XXXX, XXX, XXX−XXX

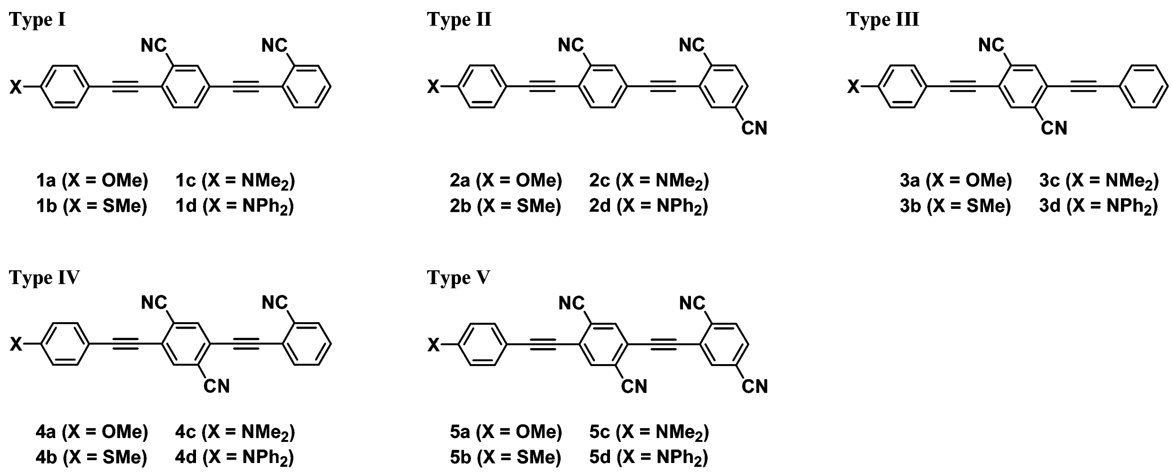

Figure 5. Molecular design for the creation of WRF.

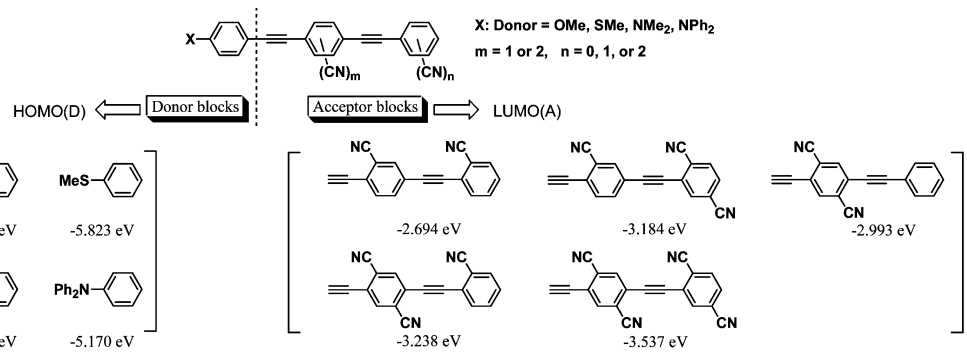

compound	Donor blocks HOMO(D)(eV)	Acceptor blocks LUMO(A)(eV)	HOMO(D)-LUMO(A) difference(eV)	Predictable λ_{em} (nm)	compound	Donor blocks tHOMO(D)(eV)	Acceptor blocks LUMO(A)(eV)	HOMO(D)-LUMO(A) difference(eV)	Predictable λ_{em} (nm)
1a	-6.068	-2.694	3.374	367	**4a**	-6.068	-3.238	2.830	438
1b	-5.823	-2.694	3.129	396	**4b**	-5.823	-3.238	2.585	480
1c	-5.143	-2.694	2.449	506	**4c**	-5.143	-3.238	1.905	651
1d	-5.170	-2.694	2.476	501	**4d**	-5.170	-3.238	1.932	642
2a	-6.068	-3.184	2.884	430	**5a**	-6.068	-3.537	2.531	490
2b	-5.823	-3.184	2.639	470	**5b**	-5.823	-3.537	2.286	542
2c	-5.143	-3.184	1.959	633	**5c**	-5.143	-3.537	1.606	772
2d	-5.170	-3.184	1.986	624	**5d**	-5.170	-3.537	1.633	759
3a	-6.068	-2.993	3.075	403					
3b	-5.823	-2.993	2.830	438					
3c	-5.143	-2.993	2.150	577					
3d	-5.170	-2.993	2.177	570					

Figure 6. Values for HOMO(D) of donor blocks, the LUMO(A) of acceptor blocks, and the HOMO(D)−LUMO(A) difference calculated by the DFT method (B3LYP/6-311G(d) level), and the predictable λ_{em} of the designed 20 D/A-BPBs (**1**−**5**).

shown in this figure, the designed D/A-BPBs are expected to emit fluorescence in the full visible region.

Synthesis of D/A-BPBs. The designed 20 D/A-BPBs (**1**−**5**) shown in Figure 5 were synthesized by way of (1) preparation of donor units (**6**−**9**) (Supporting Information), (2) preparation of acceptor units (**11**−**14**) (Supporting Information), (3) the Sonogashira Pd cross-coupling[89,90] reaction between donor units (**6**−**9**) and acceptor units (**13** or **14**), utilizing the reactivity difference between iodine and bromine on the same benzene ring, and (4) elongation of acceptor units (i.e., construction of BPB skeleton) as shown in Scheme 1.

Compounds of Type I (**1a**−**1d**) and Type II (**2a**−**2d**) containing a cyanobenzene ring as the central ring were synthesized by the first cross-coupling of donor units (**6**−**9**) with 5-bromo-2-iodobenzonitrile (**11**) followed by the second cross-coupling with 2-ethynylbenzonitrile (**13**) and 2-ethynylterephthalonitrile (**14**), respectively. The reaction of donor unit (**6**−**9**) with 5-bromo-2-iodoterephthalonitrile (**12**) at the more reactive iodo-substituted position gave **19**−**22,** followed by the second cross-coupling with ethynylbenzene (**10**) and the acceptor units (**13** and **14**) at the remaining bromo-substituted position of **19**−**22**, provided Type III (**3a**−**3d**), Type IV (**4a**−**4d**), and Type V (**5a**−**5d**), respectively. The structures of 20 D/A-BPBs were confirmed by spectral data (^{1}H and ^{13}C NMR spectroscopy and HR-FAB MS, Supporting Information).

Photophysical Properties of D/A-BPBs. Absorption and emission spectra of the synthesized D/A-BPBs (**1**−**5**) were measured in $CHCl_3$. The fluorescence spectra and photograph of emission color are illustrated in Figure 7. The photophysical data of **1**−**5** are shown in Figure 8 (A, absorption maxima, λ_{abs} (nm);

DOI: 10.1021/acs.jpca.5b05077
J. Phys. Chem. A XXXX, XXX, XXX−XXX

Scheme 1[a]

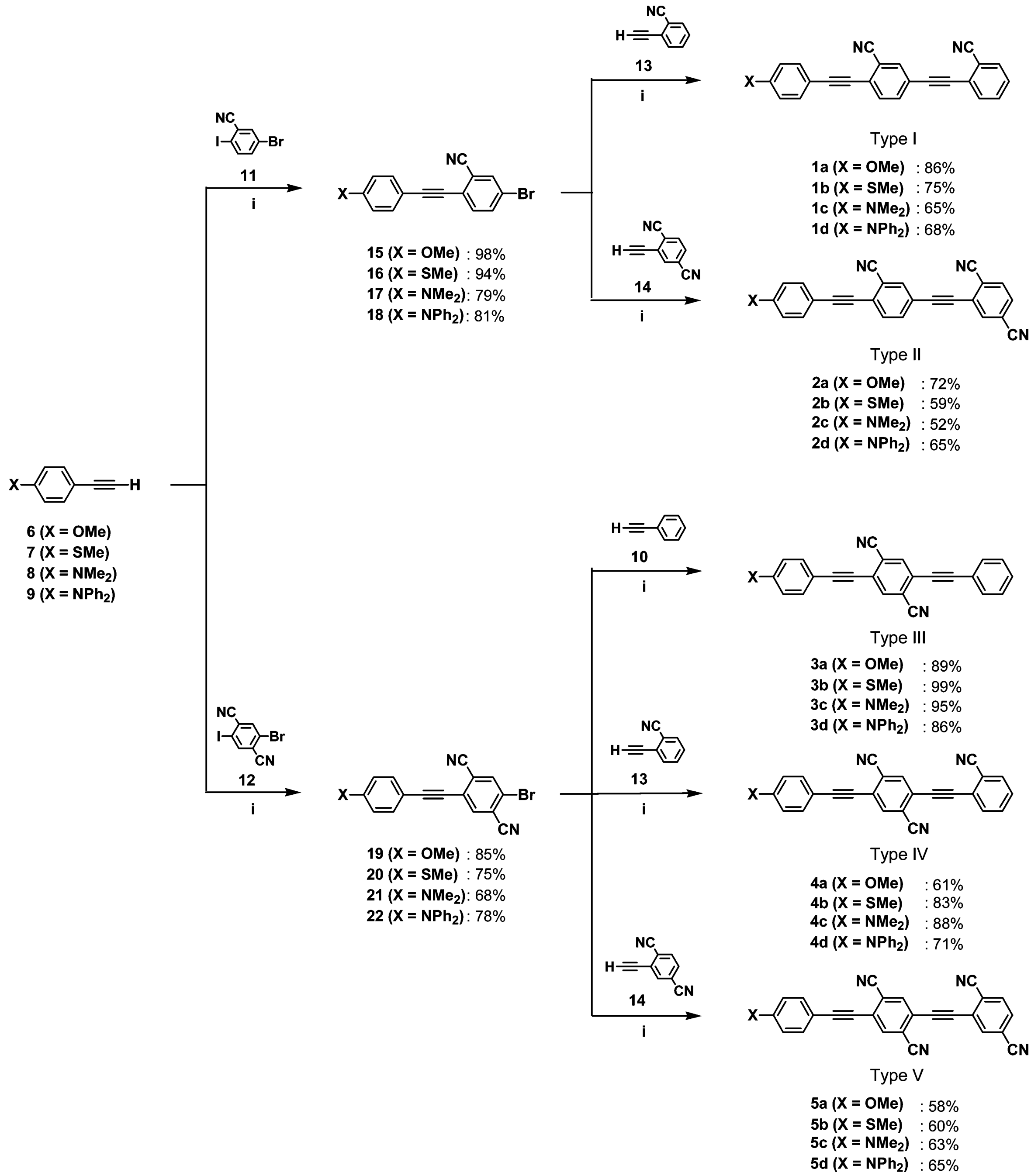

[a]Reagents: (i) $Pd(Ph_3P)_2Cl_2$, CuI, Et_3N, THF

B, emission maxima, λ_{em} (nm); C, Stokes shift (nm); D, quamtum yield, Φ_f) as three-dimensional indications (details in the Supporting Information).

As shown in Figures 7 and 8B, it is demonstrated that the synthesized D/A-BPBs (**1**−**5**) are whole-rainbow-fluorophores (WRF) having the small $\Delta\lambda_{em}$ values (almost <20 nm, Supporting Information) in the full visible region [from 409 nm (violet emission, **1a**: Type I, OMe) to 639 nm (red emission, **5d**: Type V, NPh_2)]. Furthermore, as shown in Figures 8A−C, the values of λ_{abs}, λ_{em}, and the Stokes shift increase evidently with both the structural change from Type I to Type V of acceptor unit and the change of donor group from OMe to NPh_2, indicating that λ_{abs}, λ_{em}, and Stokes shift increase with both electron-withdrawing ability of the acceptor unit and electron-donating ability of the donor groups. Such a change in Stokes shift is of particular interest. Almost all D/A-BPBs (**1**−**5**) were found to be very intense fluorophores having high quantum yield (Φ_f > 0.6, Figure 8D) and molar absorption coefficient (log ε > 4.5, Supporting Information). Thus, we succeeded in the creation of the desired WRF by using D/A-BPBs (**1**−**5**) consisting of the relatively short π-conjugated core skeleton.

Synthesis of the Intense Red Fluorophore. We succeeded in the creation of the desired WRF by synthesis of D/A-BPBs (**1**−**5**) having the BPB moiety as the short π-conjugated core skeleton, though Φ_f values of two red fluorophores (**5c** and **5d**) were lower than those of other

DOI: 10.1021/acs.jpca.5b05077
J. Phys. Chem. A XXXX, XXX, XXX−XXX

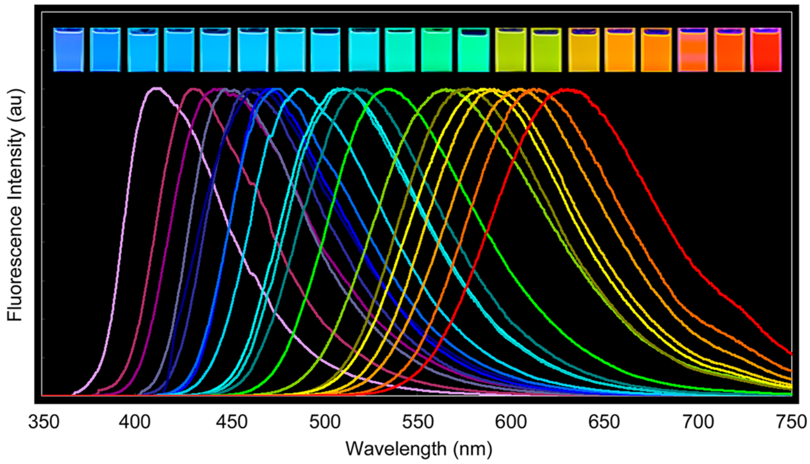

Figure 7. Fluorescence spectra and emission color of D/A-BPBs (**1**−**5**) in $CHCl_3$. Each spectrum and photograph from left to right correspond to the compound number **1a**, **1b**, **2a**, **3a**, **4a**, **2b**, **3b**, **5a**, **4b**, **5b**, **1c**, **1d**, **2c**, **2d**, **3c**, **3d**, **4c**, **4d**, **5c**, and **5d**, respectively.

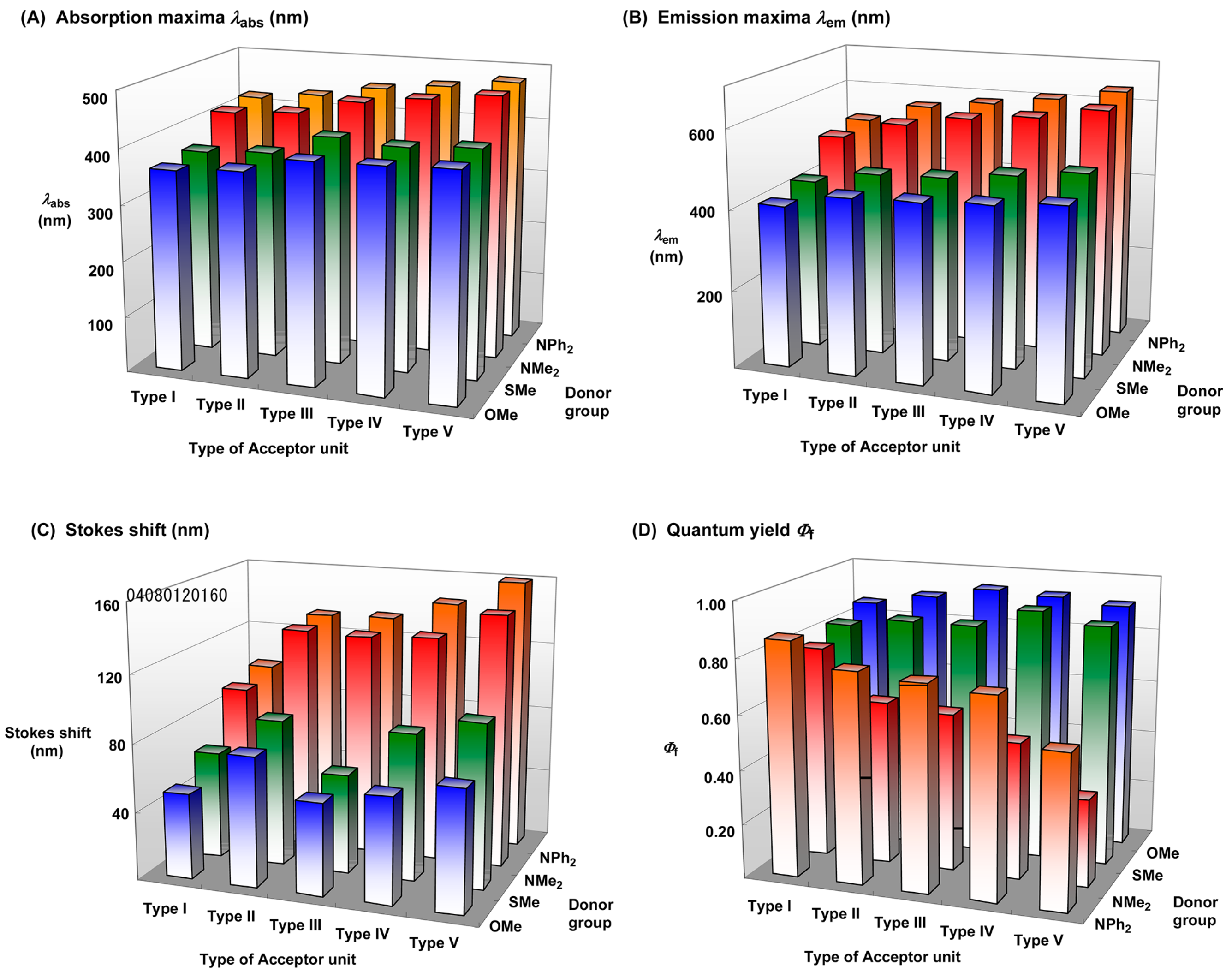

Figure 8. Photophysical data of D/A-BPBs (**1**−**5**) in $CHCl_3$ (A, absorption maxima, λ_{abs} (nm); B, emission maxima, λ_{em} (nm); C, Stokes shift (nm); D, quamtum yield, Φ_f).

fluorophores (Figure 8D). Because the balance between the electron-donating ability of the donor units and the electron-withdrawing ability of the acceptor unit has turned out to be a crucial issue for the creation of highly efficient fluorophores that emit light at the desired wavelength, five new compounds (**5e**−**5i**, Figure 9), in which the electron-donating ability is controlled by the introduction of various functional groups to the *para*-position of benzene rings of the terminal NPh_2 group of **5d**, have

DOI: 10.1021/acs.jpca.5b05077
J. Phys. Chem. A XXXX, XXX, XXX−XXX

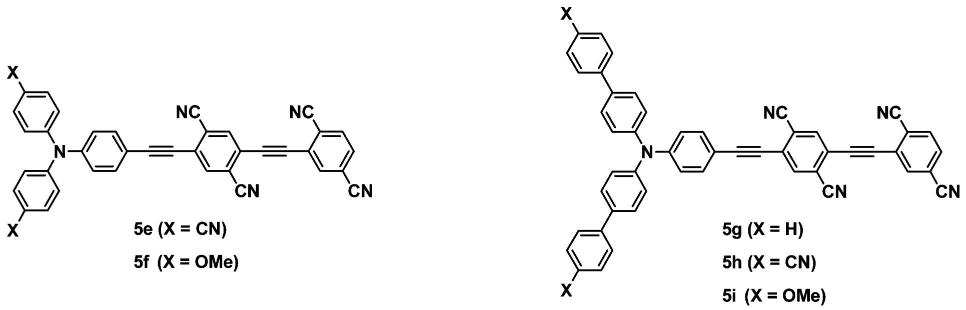

Figure 9. Structures of new compounds (**5e**−**5i**) designed for the intense red fluorophores.

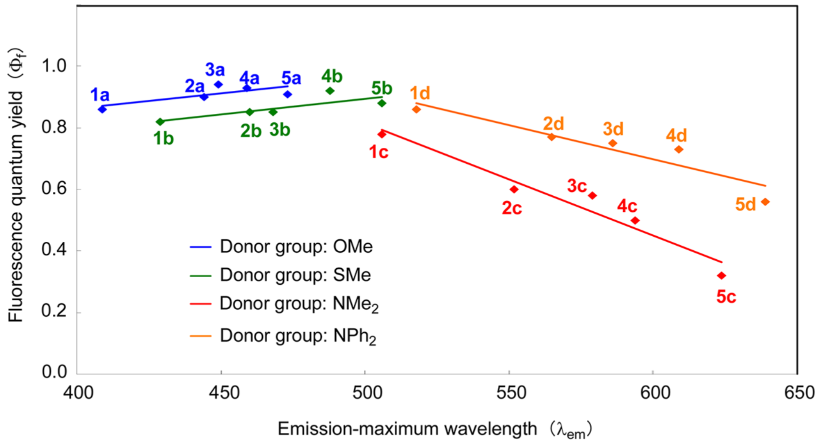

Figure 10. Relationship between Φ_f and λ_{em} of WRF (**1**−**5**).

been designed to get the intense red fluorophore ($\Phi_f > 0.7$, $\lambda_{em} >$ 610 nm).

Synthesis of **5e**−**5i** was carried out by (1) preparation of donor units and (2) sequential Pd cross-coupling reaction with two kinds of acceptor units. The synthetic method is the same as the one used in the synthesis of **5d** (details, Supporting Information). Absorption and emission spectra of the synthesized **5e**−**5i** were measured in $CHCl_3$ solution. As a result, **5h**, in which the 4-cyanophenyl group is introduced to the *para*-position of two benzene rings in the terminal NPh_2 group of **5d**, was found to emit the desired intense red fluorescence (log ε = 4.56, $\Phi_f = 0.76$, $\lambda_{em} = 611$ nm), though λ_{em} was slightly shifted to a shorter wavelength than that of **5d** ($\lambda_{em} = 639$ nm) (details in the Supporting Information).

Electronic and Spectral Features of WRF. The relationship between the emission maxima (λ_{em}) and quamtum yield (Φ_f) for WRF (**1**−**5**) was examined for each donor group (Figure 10). Interestingly, the positive linear relationships between Φ_f and λ_{em} were found for WRF (**1**−**5**) having weak electron-donating groups (OMe, **a** series; SMe, **b** series), whereas the negative linear relationships between Φ_f and λ_{em} were found for WRF (**1**−**5**) having strong electron-donating groups (NMe_2, **c** series; NPh_2, **d** series).

The observed linear relationship is closely connected with the optical energy gap law, which represents the exponential dependence of the radiationless rate constant (k_{nr}, Supporting Information)[91,92] on the energy gap between the S_1 state and the S_0 state for the fluorophores.[93−96] That is to say, the positive linear relationship between ln k_{nr} and the relevant optical energy gap (ν_{em}) in **a** and **b** series demonstrates that they do not follow the optical energy gap law, whereas the negative linear relationship between ln k_{nr} and ν_{em} in **c** and **d** series clearly indicates that they follow the law (the relationship between ln k_{nr} and ν_{em}, Supporting Information). These relations should be useful for the molecular design of novel fluorophores.

As described in the section of molecular design, we reported in the previous paper[88] that the optical transition energy (ν_{em}: cm^{-1}) from the S_1 state to the S_0 state correlates linearly with the HOMO(D)−LUMO(A) difference in the D/A-OPE system. Thus, the bathochromic shift of λ_{em} in WRF (**1**−**5**) can be explained by the degree of HOMO(D)−LUMO(A) difference. As shown in Figure 11, the relevant optical energy gap (ν_{em}) from S_1 to S_0 correlates linearly with the HOMO(D)−LUMO(A) difference (details, Supporting Information). Therefore, the fluorescence of WRF (**1**−**5**) is considered to have the high charge-transfer (CT) nature in the S_1 state.

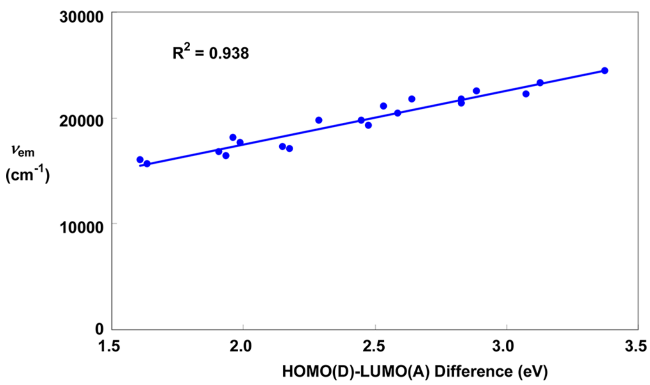

Figure 11. Relationship between ν_{em} and HOMO(D)−LUMO(A) difference calculated by DFT method (B3LYP/6-311G(d) level) in WRF (**1**−**5**).

DOI: 10.1021/acs.jpca.5b05077
J. Phys. Chem. A XXXX, XXX, XXX−XXX

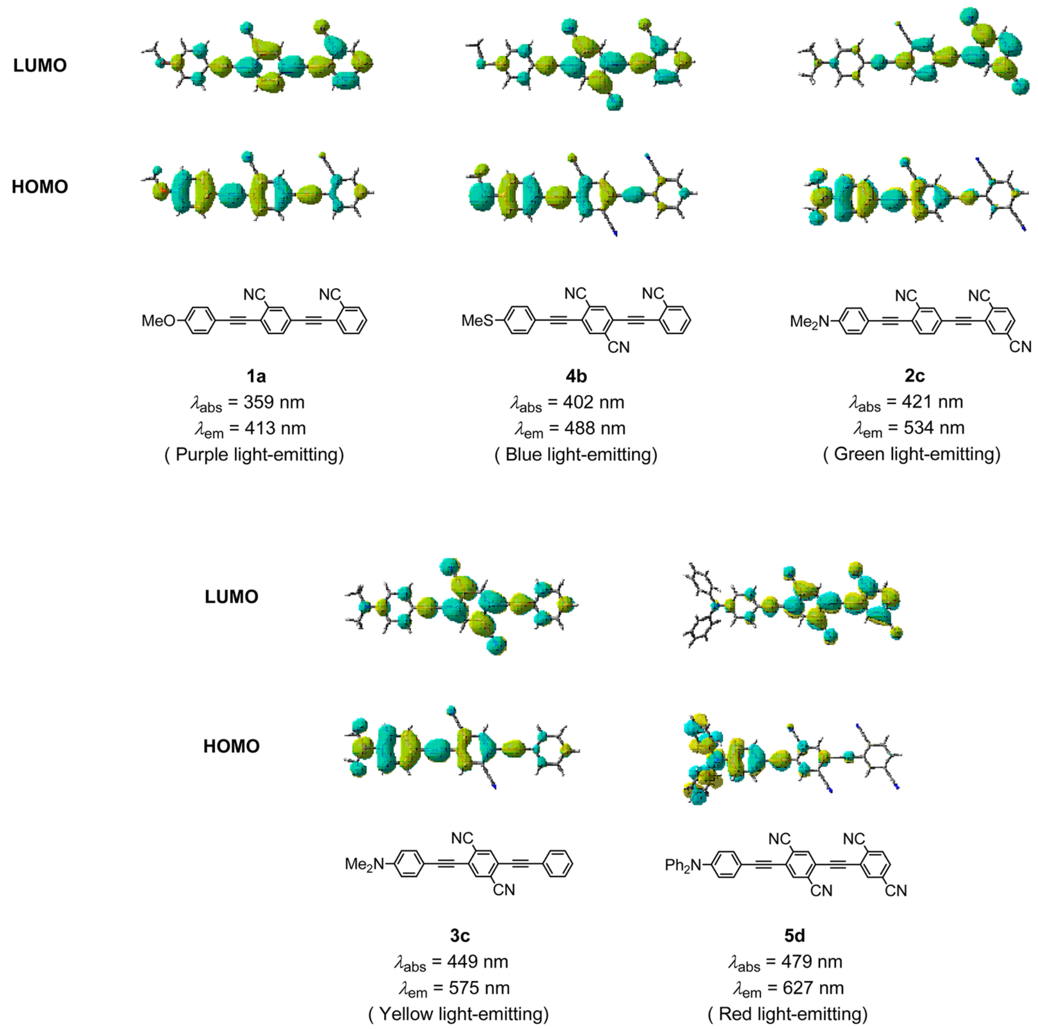

Figure 12. Molecular orbitals of **1a**, **2c**, **3c**, **4b**, and **5d** by the DFT method (B3LYP/6-311G(d) level). The upper ones represent the LUMOs, and the lower ones represent the HOMOs.

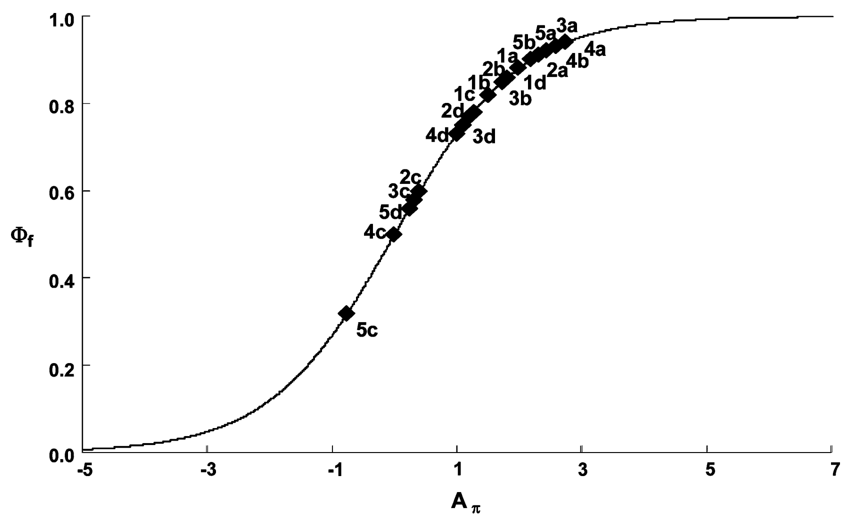

Figure 13. Correlation between absolute fluorescence quantum yield (Φ_f) and magnitude (A_π) of π conjugation length in the S_1 state of WRF (**1**−**5**). Solid line: theoretical line based on eq 1.

The high CT nature in the electronic transition of WRF (**1**−**5**) is also suggested by the quantum chemical calculations with DFT method (B3LYP/6-311G(d) level). The molecular orbitals calculated by the DFT method using the Gaussian 03 package[97] display a remarkable difference in the distribution of HOMO and LUMO in **1a**, **2c**, **3c**, **4b**, and **5d** (Figure 12).

As shown in Figure 12, the CT transition from the HOMO to the LUMO is strongly suggested to occur in **1a**, **2c**, **3c**, **4b**, and

DOI: 10.1021/acs.jpca.5b05077
J. Phys. Chem. A XXXX, XXX, XXX−XXX

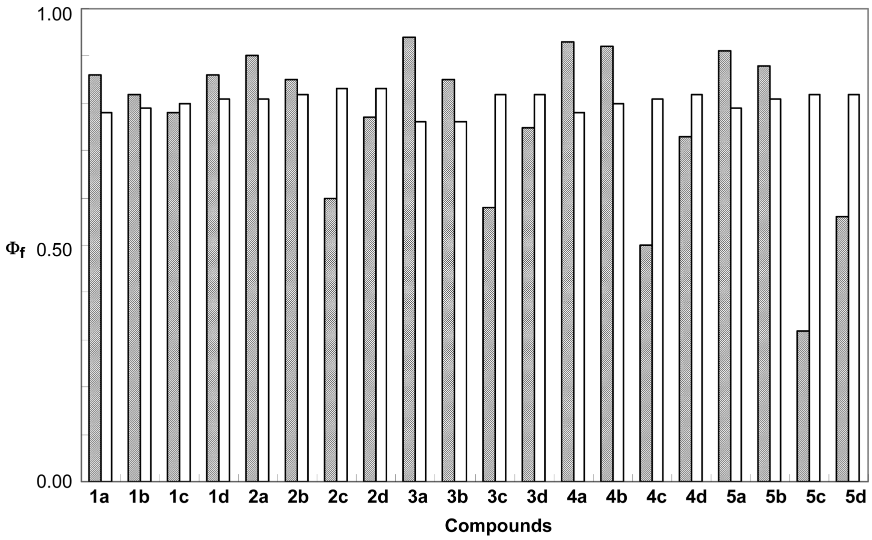

Figure 14. Observed values (Φ_f(expt), shaded bars) and predicted values (Φ_f(calcd), open bars) of Φ_f for WRF (**1–5**).

Table 1. Φ_f and λ_{em} of 1a–5i in $CHCl_3$ and 1a–5i Dispersed in PS or PMMA Film[a]

	Φ_f[b]			λ_{em} (nm)				Φ_f[b]			λ_{em} (nm)		
compd	solution	PS	PMMA	solution	PS	PMMA	compd	solution	PS	PMMA	solution	PS	PMMA
1a	0.86	0.81	0.75	409	416	415	**4a**	0.93	0.73	0.72	459	447	452
1b	0.82	0.83	0.79	429	430	431	**4b**	0.92	0.79	0.80	488	467	474
1c	0.78	0.64	0.66	506	488	506	**4c**	0.50	0.65	0.70	594	553	574
1d	0.86	0.74	0.71	518	488	500	**4d**	0.73	0.80	0.77	609	553	567
2a	0.90	0.83	0.81	444	429	431	**5a**	0.91	0.71	0.72	473	459	460
2b	0.85	0.83	0.79	460	449	448	**5b**	0.88	0.77	0.76	506	481	485
2c	0.60	0.68	0.65	569	515	543	**5c**	0.32	0.66	0.53	624	556	580
2d	0.77	0.78	0.72	565	520	525	**5d**	0.56	0.83	0.79	639	577	583
3a	0.94	0.83	0.83	449	443	448	**5e**	1.00	0.61	0.61	525	503	521
3b	0.85	0.73	0.73	468	459	467	**5f**	0.01	0.57	0.32	721	630	628
3c	0.58	0.68	0.69	579	530	561	**5g**	0.26	0.80	0.72	671	596	605
3d	0.75	0.76	0.74	586	536	552	**5h**	0.76	0.71	0.71	611	558	580
							5i	0.03	0.71	0.54	732	621	614

[a]All spectra were measured at 295 K. [b]Absolute quantum yield (Φ_f) values were determined with a Hamamatsu C9920-01 calibrated integrating sphere system.

5d, because the HOMOs are almost localized on the donor groups, whereas the LUMOs are wholly localized on acceptor units. Therefore, WRF (**1–5**) having both the donor and acceptor moiety appears to have the dipolar structure on the basis of the charge transfer[98] in the S_1 state. Consequently, the increase in interaction between WRF (**1–5**) and solvent (particularly, polar solvent) results in the increase in k_{nr} value providing a decrease in Φ_f values. Because **a** and **b** series having weak electron-donating groups (OMe and SMe) do not show such remarkable change, the CT nature stabilizes the S_1 state leading to increase in Φ_f values. However, the CT nature in **c** and **d** series having a strong electron-donating group (NMe_2 and NPh_2) increases with an increase in electron-withdrawing ability in the acceptor unit (the structural change from Type I to Type V). Therefore, although the S_1 state in **c** and **d** series is stabilized, the interaction between substrates and solvent also increases, resulting in the decrease in Φ_f values.

In our previous work,[99] the effect of π conjugation length on the fluorescence emission efficiency was elucidated by examination of theoretical and experimental relationship between Φ_f and magnitude (A_π) of π conjugation length in the S_1 state. The A_π is derived from the radiative rate constant (k_r) and radiationless rate constant (k_{nr}) [$A_\pi = \ln(k_r/k_{nr})$]. Relationship between Φ_f and A_π is expressed as eq 1.

$$\Phi_f = 1/(\exp(-A_\pi) + 1) \tag{1}$$

To see the generality of this concept, we examined the correlation between Φ_f and A_π for WRF (**1–5**) (details in the Supporting Information). As shown in Figure 13, it is of particular interest that the plot of Φ_f against A_π for WRF (**1–5**) falls on the theoretical line (solid line) based on eq 1.

For the prediction of Φ_f from a structural model, a Φ_f-independent measure is necessary, because A_π is derived from the Φ_f-dependent k_r and k_{nr}. This could be achieved by replacing A_π in eq 1 by $(\tilde{\nu}_a - \tilde{\nu}_f)^{1/2} \times a^{3/2}$ as described below: The dipole in the S_1 state is formed by light absorption (transition dipole moment). Thus, the difference ($\Delta\mu$) between the S_1 state dipole moment (μ_1) and S_0 state dipole moment (μ_0) would give a measure of the distance between the dipole, assuming that the charge in the S_1 state is close to unity, and the charge in the S_0 state is negligibly small.

The Lippert–Mataga equation is[100–102]

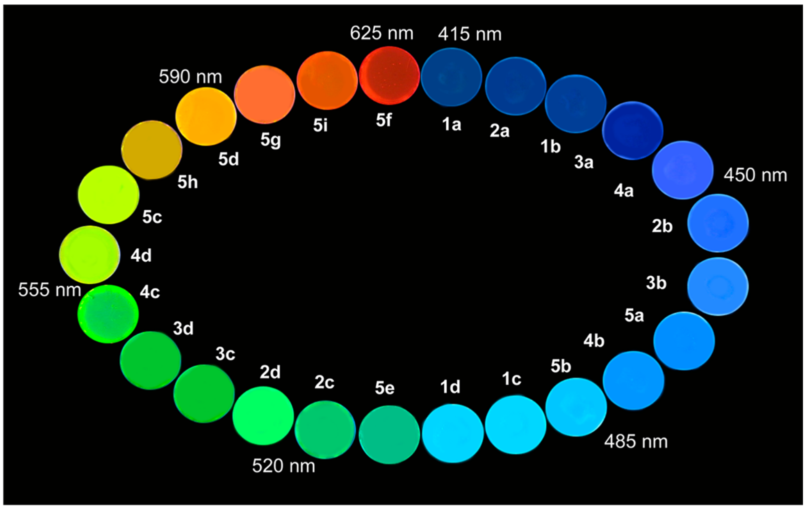

Figure 15. Emission color of **1a**−**5i** dispersed in PS film under irradiation at 254 nm.

$$\tilde{\nu}_a - \tilde{\nu}_f = \frac{2}{hc}\left(\frac{\varepsilon - 1}{2\varepsilon + 1} - \frac{n^2 - 1}{2n^2 + 1}\right)\frac{(\mu_e - \mu_g)^2}{a^3} + \text{constant} \tag{2}$$

where $\tilde{\nu}_a$ and $\tilde{\nu}_f$ are the wavenumber (cm^{-1}) of the absorption and fluorescence peaks, respectively, h is Planck's constant, c is the speed of light, ε is the dielectric constant of the solvent, n is the refractive index of the solvent, and a is the molecular radius. From eq 2,

$$\Delta\mu \propto (\tilde{\nu}_a - \tilde{\nu}_f)^{1/2} \times a^{3/2} \text{in given solvent}$$

Upon replacing A_π in eq 1 by $(\tilde{\nu}_a - \tilde{\nu}_f)^{1/2} \times a^{3/2}$, we get eq 3.

$$\Phi_f = \frac{1}{e^{(-(\tilde{\nu}_a - \tilde{\nu}_f)^{1/2} \times a^{3/2})} + 1} \tag{3}$$

In eq 3, $\tilde{\nu}_a$ and $\tilde{\nu}_f$ are observed values, and a is obtained by MM2 calculation, for example. The predicted values (Φ_f(calcd)) calculated with eq 3 and observed values (Φ_f(expt)) of Φ_f for WRF (**1**−**5**) are shown in Figure 14 (details in the Supporting Information).

Although some deviation [$\Delta\Phi_f = \Phi_f(\text{expt}) - \Phi_f(\text{calcd})$] is seen between the calculated values (Φ_f(calcd)) and the experimental values (Φ_f(expt)) (Figure 14), the values calculated with eq 3 agree very closely with the experimental values except for **2c** ($\Delta\Phi_f = -0.23$), **3c** ($\Delta\Phi_f = -0.24$), **4c** ($\Delta\Phi_f = -0.29$), **5c** ($\Delta\Phi_f = -0.50$), and **5d** ($\Delta\Phi_f = -0.26$), where both the strong electron-donating groups (NMe_2 and NPh_2) and the strong electron-withdrawing acceptor units (Type IV and Type V) exist.

Light-Emitting Properties of Doped Polymer Films. From the viewpoint of application of WRF to various functional materials, the elucidation of light-emitting characteristics in solution alone is not satisfactory; accordingly, light-emitting characteristics of **1a**−**5i** in doped polymer films was examined as the fundamental experiment for application. **1a**−**5i** dispersed in polymer film were prepared by mixing each compound and polystyrene (PS) or poly(methyl methacrylate) (PMMA) in THF, followed by spin-coating. The light-emitting characteristics for **1a**−**5i** dispersed in polymer film were measured. The obtained results together with the relating data in $CHCl_3$ solution are summarized in Table 1. The emission photographs of **1a**−**5i** dispersed in PS film under irradiation at 254 nm are shown in Figure 15.

As shown in Table 1, emission maxima (λ_{em}) of D/A-BPBs (**1a**−**5i**) in both polymer films are significantly blue-shifted from those in $CHCl_3$ solution. Because the concentration of D/A-BPBs (**1a**−**5i**) in films (ca. 10^{-2} M) is higher than that in solution (ca. 10^{-6} M), the association of compounds is expected to occur in films. D/A-type compounds are known to form a H-type or J-type association in high concentrated state to result in a blue shift or red shift of λ_{abs}. Thus, the significant blue shift of λ_{em} in both polymer films indicates a H-type coupling of D/A-BPBs (**1a**−**5i**) in both films, because the Stokes shift does not change much in both solution and polymer. As shown in Table 1 and Figure 15, it is demonstrated that **1a**−**5i** dispersed in polymer film emit light at the whole visible region (from 416 nm (**1a**) to 630 nm (**5f**) in PS, from 415 nm (**1a**) to 628 nm (**5f**) in PMMA) and have the small $\Delta\lambda_{em}$ values (<20 nm, except for $\Delta\lambda_{em}$ (between **5g** and **5i**) = 25 nm in PS and $\Delta\lambda_{em}$ (between **5d** and **5g**) = 22 nm in PMMA). Furthermore, **1a**−**5i** dispersed in polymer film is seen to have high Φ_f values (>0.6) in almost all cases (except for **5f** in PS and **5c**, **5f**, **5i** in PMMA) and log ε values (>4.5) in all cases regardless of the kind of polymer used. Therefore, D/A-BPBs (**1a**−**5i**) can be mentioned to be the desired WRF in doped polymer film also.

Although the λ_{em} values of WRF (**1a**−**5i**) dispersed in polymer film were smaller than those observed in $CHCl_3$ solution, it is worth noting that the Φ_f values of **5c**, **5f**, **5g**, and **5i** dispersed in polymer film increase dramatically compared with those in $CHCl_3$ solution. Thus, the superior light-emitting properties of WRF (**1a**−**5i**) dispersed in polymer film would enable the various application to functional materials.

■ CONCLUSION

In conclusion, we synthesized 20 D/A-BPBs (**1**−**5**), which are expected to emit light in the full visible region on the basis of the positive linear relationship between ν_{em} and the HOMO(D)−LUMO(A) difference calculated by DFT method, by devising the favorable reaction conditions, and disclosed their fluorescence emission characteristics in $CHCl_3$ solution and in doped polymer film. Consequently, it has been demonstrated that D/A-BPBs (**1**−**5**) are the desired WRF (whole-rainbow-fluorophores) that emit light in full visible region (400 nm < λ_{em} > 650 nm) and have the small $\Delta\lambda_{em}$ (the difference of λ_{em} between a given fluorophore and nearest neighboring fluorophore having

DOI: 10.1021/acs.jpca.5b05077
J. Phys. Chem. A XXXX, XXX, XXX−XXX

the same core skeleton) values (<20 nm), the high log ε values (>4.5), and the high Φ_f values (>0.6).

We synthesized five new compounds (**5e**−**5i**) to get the intense red fluorophore ($\Phi_f > 0.7$, $\lambda_{em} > 610$ nm) and elucidated their photophysical proterties in $CHCl_3$ solution. As a result, **5h**, in which the 4-cyanophenyl group is introduced to the *para*-position of two benzene rings in the terminal NPh_2 group of **5d**, was found to be the desired intense red fluorophore (log ε = 4.56, Φ_f = 0.76, λ_{em} = 611 nm).

Finding on the positive linear relationships between Φ_f and λ_{em} for WRF (**1**−**5**) with the weak electron-donating group (OMe, **a** series; SMe, **b** series) is of interest. We elucidated the intramolecular charge-transfer nature of the S_1 state of WRF (**1**−**5**) by a positive linear relationship between the optical transition energy (ν_{em}) from the S_1 state to the S_0 state and the HOMO(D)−LUMO(A) difference, and the molecular orbitals calculated with the DFT method. It is demonstrated that our concept ($\Phi_f = 1/(\exp(-A_\pi) + 1)$) connected with the relationship between Φ_f and magnitude (A_π) of π conjugation length in the S_1 state can be applied to WRF (**1**−**5**). This concept should be valuable for examination of an S_1 state structure.

Moreover, it is suggested that the prediction of Φ_f from a structural model can be achieved by the equation $\Phi_f = 1/(\exp(-((\tilde{\nu}_a - \tilde{\nu}_f)^{1/2} \times a^{3/2}) + 1)$, where $\tilde{\nu}_a$ and $\tilde{\nu}_f$ are the wavenumber (cm^{-1}) of the absorption and fluorescence peaks, respectively, and *a* is the calculated molecular radius. Although some deviation is seen in the optical gap between the calculated values and the experimental values, almost all the values calculated with the equation $\Phi_f = 1/(\exp(-((\tilde{\nu}_a - \tilde{\nu}_f)^{1/2} \times a^{3/2}) + 1)$ are in agreement with the experimental values.

Finally, from the viewpoint of application of WRF to various functional materials, the light-emitting characteristics of **1a**−**5i** in doped polymer films was examined. As a result, it was demonstrated that **1a**−**5i** dispersed in two kinds of polymer film (PS and PMMA) emit light at the whole visible region and have small $\Delta\lambda_{em}$ values (<20 nm) and high Φ_f values (>0.6). Therefore, D/A-BPBs (**1a**−**5i**) are also to be the desired WRF even in the doped polymer film, and the superior light-emitting properties of WRF (**1a**−**5i**) dispersed in polymer film are quite useful in view of their application to various functional materials.

■ ASSOCIATED CONTENT

Supporting Information

Description of equipment and methods, synthetic procedures and product characterization data, absorption spectra, photophysical data, the relationship between $\ln k_{nr}$ and ν_{em}, the comparison of predictable λ_{em} and experimental λ_{em}, A_π values, practical A_π (A_π*), and the comparison of predictable Φ_f and experimental Φ_f. The Supporting Information is available free of charge on the ACS Publications website at DOI: 10.1021/acs.jpca.5b05077.

■ AUTHOR INFORMATION

Corresponding Authors

*Y. Yamaguchi. E-mail: yamaguch@chem.kindai.ac.jp.

*Z. Yoshida. E-mail: yoshida@chem.kindai.ac.jp.

Notes

The authors declare no competing financial interest.

■ ACKNOWLEDGMENTS

This work was supported by Ministry of Education, Culture, Sports, Science and Technology (MEXT)−Supported Program for the Strategic Research Foundation at Private Universities, 2014−2018).

■ REFERENCES

(1) Rasmussen, S. C.; Evenson, S. J.; McCaysland, C. B. Fluorescent Thiophene-Based Materials and Their Outlook for Emissive Applications. *Chem. Commun.* **2015**, *51*, 4528−4543.

(2) Ni, Y.; Zeng, L.; Kang, N.-Y.; Huang, K.-W.; Wang, L.; Zeng, Z.; Chang, Y.-T.; Wu, J. Meso-Ester- and Carboxylic-Acid-Substituted BODIPYs with Far-Red and Near-Infrared Emission for Bioimaging Applications. *Chem. - Eur. J.* **2014**, *20*, 2301−2310.

(3) Goncalves, M. S. T. Fluorescent Labeling of Biomolecules with Organic Probes. *Chem. Rev.* **2009**, *109*, 190−212.

(4) Nolan, E. M.; Lippard, S. J. Tools and Tactics for the Optical Detection of Mercuric Ion. *Chem. Rev.* **2008**, *108*, 3443−3480.

(5) Thompson, R. B. *Fluorescence Sensors and Biosensors*; CRC Press LLC: Boca Raton, FL, 2006.

(6) Yoshimoto, K.; Nishizawa, S.; Minagawa, M.; Teramae, N. Use of Abasic Site-Containing DNA Strands for Nucleobase Recognition in Water. *J. Am. Chem. Soc.* **2003**, *125*, 8982−8983.

(7) Lavigne, J. J.; Anslyn, E. V. Sensing a Paradigm Shift in the Field of Molecular Recognition: from Selective to Differential Receptors. *Angew. Chem., Int. Ed.* **2001**, *40*, 3118−3130.

(8) Zhang, Q.; Li, B.; Huang, S.; Nomura, H.; Tanaka, H.; Adachi, C. Efficient Blue Organic Light-Emitting Diodes Employing Thermally Activated Delayed Fluorescence. *Nat. Photonics* **2014**, *8*, 326−332.

(9) Shuto, A.; Kushida, T.; Fukushima, T.; Kaji, H.; Yamaguchi, S. π-Extended Planarized Triphenylboranes with Thiophene Spacers. *Org. Lett.* **2013**, *15*, 6234−6237.

(10) Uoyama, H.; Goushi, K.; Shizu, K.; Nomura, H.; Adachi, C. Highly Efficient Organic Light-Emitting Diodes from Delayed Fluorescence. *Nature* **2012**, *492*, 234−238.

(11) Wang, E.; Li, C.; Zhuang, W.; Peng, J.; Cao, Y. High-Efficiency Red and Green Light-Emitting Polymers Based on a Novel Wide Bandgap Poly(2,7-silafluorene). *J. Mater. Chem.* **2008**, *18*, 797−801.

(12) Yersin, H. *Highly Efficient OLEDs with Phosphorescent Materials*; Wiley-VCH: Weinheim, 2008.

(13) Sanchez, J. C.; DiPasquale, A. G.; Rheingold, A. L.; Trogler, W. C. Synthesis, Luminescence Properties, and Explosives Sensing with 1,1-Tetraphenylsilole- and 1,1-Silafluorene-vinylene Polymers. *Chem. Mater.* **2007**, *19*, 6459−6470.

(14) Kato, S.-i.; Furuya, T.; Kobayashi, A.; Nitani, M.; Ie, Y.; Aso, Y.; Yoshihara, T.; Tobita, S.; Nakamura, Y. π-Extended Thiadiazoles Fused with Thienopyrrole or Indole Moieties: Synthesis, Structures, and Properties. *J. Org. Chem.* **2012**, *77*, 7595−7606.

(15) Beaujuge, P. M.; Pisula, W.; Hoi, N. T.; Ellinger, S.; Müllen, K.; Reynolds, J. R. Tailoring Structure-Property Relationships in Dithienosilole-Benzothiadiazole Donor-Acceptor Copolymers. *J. Am. Chem. Soc.* **2009**, *131*, 7514−7515.

(16) Grimsdale, A. C.; Chan, K. L.; Martin, R. E.; Jokisz, P. G.; Holmes, A. B. Synthesis of Light-Emitting Conjugated Polymers for Applications in Electroluminescent Devices. *Chem. Rev.* **2009**, *109*, 897−1091.

(17) Lu, G.; Usta, H.; Risko, C.; Wang, L.; Facchetti, A.; Ratner, M. A.; Marks, T. J. Synthesis, Characterization, and Transistor Response of Semiconducting Silole Polymers with Substantial Hole Mobility and Air Stability. Experiment and Theory. *J. Am. Chem. Soc.* **2008**, *130*, 7670−7685.

(18) Shimizu, S.; Iino, T.; Saeki, A.; Seki, S.; Kobayashi, N. Rational Molecular Design towards Vis/NIR Absorption and Fluorescence by Using Pyrrolopyrrole aza-BODIPY and Its Highly Conjugated Structures for Organic Photovoltaics. *Chem. - Eur. J.* **2015**, *21*, 2893−2904.

(19) Kranthiraja, K.; Gunasekar, K.; Cho, W.; Song, M.; Park, Y. G.; Lee, J. Y.; Shin, Y.; Kang, I.-N.; Kim, A.; Kim, H.; et al. Alkoxyphenylthiophene Linked Benzodithiophene Based Medium Band Gap Polymers for Organic Photovoltaics: Efficiency Improvement upon Methanol Treatment Depends on the Planarity of Backbone. *Macromolecules* **2014**, *47*, 7060−7069.

DOI: 10.1021/acs.jpca.5b05077
J. Phys. Chem. A XXXX, XXX, XXX−XXX

(20) Senevirathna, W.; Sauvě, G. Introducing 3D Conjugated Acceptors with Intense Red Absorption: Homoleptic Metal(II) Complexes of Di(phenylacetylene) azadipyrromethene. *J. Mater. Chem. C* **2013**, *1*, 6684−6694.

(21) Mullenebach, T. K.; McGarry, K. A.; Luhman, W. A.; Douglas, C. J.; Holmes, R. J. Connecting Molecular Structure and Exciton Diffusion Length in Rubrene Derivatives. *Adv. Mater.* **2013**, *25*, 3689−3693.

(22) Nia, A. S.; Enders, C.; Binder, W. H. Hydrogen-Bonded Perylene/Terthiophene-Materials: Synthesis and Spectroscopic Properties. *Tetrahedron* **2012**, *68*, 722−729.

(23) Zou, Y.; Gendron, D.; Neagu-Plesu, R.; Leclerc, M. Synthesis and Characterization of New Low-Bandgap Diketopyrrolopyrrole-Based Copolymers. *Macromolecules* **2009**, *42*, 6361−6365.

(24) Hou, J.; Chen, H. Y.; Zhang, S.; Li, G.; Yang, Y. Synthesis, Characterization, and Photovoltaic Properties of a Low Band Gap Polymer Based on Silole-Containing Polythiophenes and 2,1,3-Benzothiadiazole. *J. Am. Chem. Soc.* **2008**, *130*, 16144−16145.

(25) Shimizu, M.; Takeda, Y.; Higashi, M.; Hiyama, T. 1,4-Bis(alkenyl)-2,5-dipiperidinobenzenes: Minimal Fluorophores Exhibiting Highly Efficient Emission in the Solid State. *Angew. Chem., Int. Ed.* **2009**, *48*, 3653−3656.

(26) Jiu, T.; Li, Y.; Liu, H.; Ye, J.; Liu, X.; Jiang, L.; Yuan, M.; Li, J.; Li, C.; Wang, S.; et al. Brightly Full-Color Emissions of Oligo(*p*-phenylenevinylene)s: Substituent Effects on Photophysical Properties. *Tetrahedron* **2007**, *63*, 3168−3172.

(27) Hwang, G. T.; Son, H. S.; Ku, J. K.; Kim, B. H. Synthesis and Photophysical Studies of Bis-enediynes as Tunable Fluorophores. *J. Am. Chem. Soc.* **2003**, *125*, 11241−11248.

(28) Zhao, D.; Li, G.; Wu, D.; Qim, X.; Neuhaus, P.; Cheng, Y.; Yang, S.; Lu, Z.; Pu, X.; Long, C.; et al. Regiospecific *N*-Heteroarylation of Amidines for Full-Color-Tunable Boron Difluoride Dyes with Mechanochromic Luminescence. *Angew. Chem., Int. Ed.* **2013**, *52*, 13676−13680.

(29) Umezawa, K.; Nakamura, Y.; Makino, H.; Citterio, D.; Suzuki, K. Bright, Color-Tunable Fluorescent Dyes in the Visible-Near-Infrared Region. *J. Am. Chem. Soc.* **2008**, *130*, 1550−1551.

(30) Wakamiya, A.; Mori, K.; Yamaguchi, S. 3-Boryl-2,2′-bithiophene as a Versatile Core Skeleton for Full-Color Highly Emissive Organic Solids. *Angew. Chem., Int. Ed.* **2007**, *46*, 4273−4276.

(31) Loudet, A.; Burgess, K. BODIPY Dyes and Their Derivatives: Syntheses and Spectroscopic Properties. *Chem. Rev.* **2007**, *107*, 4891−4932.

(32) Shimizu, M.; Mochida, K.; Katoh, M.; Hiyama, T. Synthesis and Photophysical Properties of 2-Donor-7-acceptor-9-silafluorenes: Remarkable Fluorescence Solvatochromism and Highly Efficient Fluorescence in Doped Polymer Films. *J. Phys. Chem. C* **2010**, *114*, 10004−10014.

(33) Kim, E.; Koh, M.; Lim, B. J.; Park, S. B. Emission Wavelength Prediction of a Full-Color-Tunable Fluorescent Core Skeleton, 9-Aryl-1,2-dihydropyrrolo[3,4-b]indolizin-3-one. *J. Am. Chem. Soc.* **2011**, *133*, 6642−6649.

(34) Kim, E.; Park, S. B. Chemistry as a Prism: A Review of Light-Emitting Materials Having Tunable Emission Wavelengths. *Chem. - Asian J.* **2009**, *4*, 1646−1658.

(35) Kim, E.; Koh, M.; Ryu, J.; Park, S. B. Combinatorial Discovery of Full-Color-Tunable Emissive Fluorescent Probes Using a Single Core Skeleton, 1,2-Dihydropyrrolo[3,4-β]indolizin-3-one. *J. Am. Chem. Soc.* **2008**, *130*, 12206−12207.

(36) Lee, S. C.; Park, S. B. Novel Application of Leuckart-Wallach Reaction for Synthesis of Tetrahydro-1,4-benzodiazepin-5-ones Library. *Chem. Commun.* **2007**, 3714−3716.

(37) Zhang, H.; Shan, X.; Zhou, L.; Lim, P.; Li, R.; Ma, E.; Guo, X. J.; Du, S. Full-Colour Fluorescent Materials Based on Mixed-Lanthanide-(III) Metal-Organic Complexes with High-Efficiency White Light Emission. *J. Mater. Chem. C* **2013**, *1*, 888−891.

(38) Liao, S. H.; Shiu, J. R.; Liu, S. W.; Yeh, S. J.; Chen, Y. H.; Chen, C. T.; Chow, T. J.; Wu, C. I. Hydroxynaphthyridine-Derived Group III Metal Chelates: Wide Band Gap and Deep Blue Analogues of Green Alq3 (Tris(8-hydroxyquinolate)aluminum) and Their Versatile Applications for Organic Light-Emitting Diodes. *J. Am. Chem. Soc.* **2009**, *131*, 763−777.

(39) Avilov, I.; Minoofar, P.; Cornil, J.; Cola, L. D. Influence of Substituents on the Energy and Nature of the Lowest Excited States of Heteroleptic Phosphorescent Ir(III) Complexes: A Joint Theoretical and Experimental Study. *J. Am. Chem. Soc.* **2007**, *129*, 8247−8258.

(40) Montes, V. A.; Pohl, R.; Shinar Anzenbacher, J., Jr. Effective Manipulation of the Electronic Effects and Its Influence on the Emission of 5-Substituted Tris(8-quinolinolate) Aluminum(III) Complexes. *Chem. - Eur. J.* **2006**, *12*, 4523−4535.

(41) Lin, B. C.; Cheng, C. P.; You, Z. Q.; Hsu, C. P. Charge Transport Properties of Tris(8-hydroxyquinolinato)aluminum(III): Why It Is an Electron Transporter. *J. Am. Chem. Soc.* **2005**, *127*, 66−67.

(42) Tamayo, A. B.; Alleyne, B. D.; Djurovich, P. I.; Lamansky, S.; Tsyba, I.; Ho, N. N.; Bau, R.; Thompson, M. E. Synthesis and Characterization of Facial and Meridional Tris-cyclometalated Iridium-(III) Complexes. *J. Am. Chem. Soc.* **2003**, *125*, 7377−7387.

(43) Lee, S. Y.; Yasuda, T.; Yang, Y. S.; Zhang, Q.; Adachi, C. Luminous Butterflies: Efficient Exciton Harvesting by Benzophenone Derivatives for Full-Color Delayed Fluorescence OLEDs. *Angew. Chem., Int. Ed.* **2014**, *53*, 6402−6406.

(44) Chen, B.; Yu, G.; Li, X.; Ding, Y.; Wang, C.; Liu, Z.; Xie, Y. Full-Color Luminescent Compounds Based on Anthracene and 2,2′-Dipyridylamine. *J. Mater. Chem. C* **2013**, *1*, 7409−7417.

(45) Khanasa, T.; Prachumrah, N.; Rattanawan, R.; Jungsuttiwong, S.; Keawin, T.; Sudyoadsuk, T.; Tuntulami, T.; Promarak, V. Bis(carbazol-9-ylphenyl)aniline End-Capped Oligoarylenes as Solution-Processed Nondoped Emitters for Full-Emission Color Tuning Organic Light-Emitting Diodes. *J. Org. Chem.* **2013**, *78*, 6702−6713.

(46) Babu, S. S.; Hollamby, M. J.; Aimi, J.; Ozawa, H.; Saeki, A.; Seki, S.; Kobayashi, K.; Hagiwara, K.; Yoshizawa, M.; Möhwald, H.; et al. Nonvolatile Liquid Anthracenes for Facile Full-Color Luminescence Tuning at Single Blue-Light Excitation. *Nat. Commun.* **2013**, *4*, 2969.

(47) Yao, D.; Zao, S.; Guo, J.; Zhang, Z.; Zhang, H.; Liu, Y.; Wang, Y. Hydroxyphenyl-Benzothiazole Based Full Color Organic Emitting Materials Generated by Facile Molecular Modification. *J. Mater. Chem.* **2011**, *21*, 3568−3570.

(48) Adachi, N.; Itagaki, R.; Sugeno, M.; Norioka, T. Dispersion of Fullerene in Neat Synthesized Liquid-State Oligo(*p*-phenyleneethynylene)s. *Chem. Lett.* **2014**, *43*, 1770−1772.

(49) Lin, C.-J.; Kundu, K. K.; Lin, C.-K.; Yang, J.-S. Conformational Control of Oligo(p-phenyleneethynylene)s with Intrinsic Substituent Electronic Effects: Origin of the Twist in Pentiptycene-Containing Systems. *Chem. - Eur. J.* **2014**, *20*, 14826−14833.

(50) Duvanel, G.; Grilj, J.; Vauthey, E. Ultrafast Long-Distance Excitation Energy Transport in Donor-Bridge-Acceptor Systems. *J. Phys. Chem. A* **2013**, *117*, 918−928.

(51) Florian, A.; Mayoral, M. J.; Stepanenko, V.; Fernández, G. Alternated Stacks of Nonpolar Oligo(p-phenyleneethynylene)-BODIPY Systems. *Chem. - Eur. J.* **2012**, *18*, 14957−14961.

(52) Zhu, N.; Yan, Q.; Luo, Z.; Zhai, Y.; Zhao, D. Helical Folding of Conjugated Oligo(phenyleneethynylene): Chain-Length Dependence, Solvent Effects, and Intermolecular Assembly. *Chem. - Asian J.* **2012**, *7*, 2386−2393.

(53) Tang, Y.; Hill, E. H.; Zhou, Z.; Evans, D. G.; Schanze, K. S.; Whitten, D. G. Synthesis, Self-Assembly, and Photophysical Properties of Cationic Oligo(*p*-phenyleneethynylene)s. *Langmuir* **2011**, *27*, 4945−4955.

(54) Maag, D.; Kottke, T.; Schlute, M.; Dodt, A. Synthesis of Monodisperse Oligo(1,4-phenyleneethynylene-alt-1,4-triptycyleneethynylene)s. *J. Org. Chem.* **2009**, *74*, 7733−7742.

(55) Ochi, T.; Yamaguchi, Y.; Wakamiya, T.; Matsubara, Y.; Yoshida, Z. Block Modification of Rod-Shaped π Conjugated Carbon Frameworks with Donor and Acceptor Groups toward Highly Fluorescent Molecules: Synthesis and Emission Characteristics. *Org. Biomol. Chem.* **2008**, *6*, 1222−1231.

(56) Shi, Z.-F.; Wang, L.-J.; Wang, H.; Cao, X.-P.; Zhang, H.-L. Synthesis of Oligo(phenylene ethynylene)s with Dendrimer "Shells" for Molecular Electronics. *Org. Lett.* **2007**, *9*, 595−598.

(57) Zucchero, A. J.; Wilson, J. N.; Bunz, U. H. F. Cruciforms as Functional Fluorophores: Response to Protons and Selected Metal Ions. *J. Am. Chem. Soc.* **2006**, *128*, 11872−11881.

(58) Bhaskar, A.; Ramakrishna, G.; Lu, Z.; Twieg, R.; Hales, J. M.; Hagan, D. J.; Stryland, E. V.; Goodson, T., III. Investigation of Two-Photon Absorption Properties in Branched Alkene and Alkyne Chromophores. *J. Am. Chem. Soc.* **2006**, *128*, 11840−11849.

(59) Yamaguchi, Y.; Kobayashi, S.; Wakamiya, T.; Matsubara, Y.; Yoshida, Z. Banana-Shaped Oligo(aryleneethynylene)s: Synthesis and Light-Emitting Characteristics. *Angew. Chem., Int. Ed.* **2005**, *44*, 7040−7044.

(60) Jana, D.; Ghorai, B. K. Hexaphenylbenzene End-Capped Tri(*p*-phenylenevinylenes): Synthesis and Properties. *Tetrahedron Lett.* **2014**, *55*, 5203−5206.

(61) Yao, C.; Lu, Q.; Wang, X.; Wang, F. Reversible Sol-Gel Transition of Oligo(*p*-phenylenevinylene)s by *π*-*π* Stacking and Dissociation. *J. Phys. Chem. B* **2014**, *118*, 4661−4668.

(62) Yagai, S.; Ishiwatari, K.; Lim, X.; Karatsu, T.; Kitamura, A.; Uemura, S. Rational Design of Photoresponsive Supramolecular Assemblies Based on Diarylethene. *Chem. - Eur. J.* **2013**, *19*, 6971−6975.

(63) Mizusaki, M.; Yamada, Y.; Obara, S.; Tada, K. Synthesis of *π*-Conjugated Two Generation Dendrimer Composed of *p*-Phenylenevinylene Dendron and Triphenylamine Surface Group. *Chem. Lett.* **2012**, *41*, 516−517.

(64) Babu, S. S.; Aimi, J.; Ozawa, H.; Shirahata, N.; Saeki, A.; Seki, S.; Ajayaghosh, A.; Möhwald, H.; Nakanishi, T. Solvent-Free Luminescent Organic Liquids. *Angew. Chem., Int. Ed.* **2012**, *51*, 3391−3395.

(65) Vijayakumar, C.; Praveen, V. K.; Kartha, K. K.; Ajayaghosh, A. Excitation Energy Migration in Oligo(*p*-phenylenevinylene) Based Organogels: Structure-Property Relationship and FRET Efficiency. *Phys. Chem. Chem. Phys.* **2011**, *13*, 4942−4949.

(66) Fang, H.-H.; Chen, Q.-D.; Yang, J.; Xia, H.; Gao, B.-R.; Feng, J.; Ma, Y.-G.; Sun, H.-B. Two-Photon Pumped Amplified Spontaneous Emission from Cyano-Substituted Oligo(*p*-phenylenevinylene) Crystals with Aggregation-Induced Emission Enhancement. *J. Phys. Chem. C* **2010**, *114*, 11958−11961.

(67) Sharma, A.; Sharma, N.; Kumar, R.; Shard, A.; Sinha, A. K. Direct Olefination of Benzaldehydes into Hydroxy Functionalized Oligo(*p*-phenylenevinylene)s via Pd-Catalyzed Heterodomino Knoevenagel-Decarboxylation-Heck Sequence and Its Application for Fluoride Sensing *π*-Conjugated Units. *Chem. Commun.* **2010**, *46*, 3283−3285.

(68) Nishizawa, T.; Lim, H. K.; Tajima, K.; Hashimoto, K. Highly Uniaxial Orientation in Oligo(*p*-phenylenevinylene) Films Induced During Wet-Coating Process. *J. Am. Chem. Soc.* **2009**, *131*, 2464−2465.

(69) He, G. S.; Tan, L. S.; Zheng, Q.; Prasad, P. N. Multiphoton Absorbing Materials: Molecular Designs, Characterizations, and Applications. *Chem. Rev.* **2008**, *108*, 1245−1330.

(70) Ajayaghosh, A.; Vijayakumar, C.; Praveen, V. K.; Babu, S. S.; Varghese, R. Self-Location of Acceptors as ″Isolated″ or ″Stacked″ Energy Traps in a Supramolecular Donor Self-Assembly: A Strategy to Wavelength Tunable FRET Emission. *J. Am. Chem. Soc.* **2006**, *128*, 7174−7175.

(71) Liang, T. T.; Naitoh, Y.; Horikawa, M.; Ishida, T.; Mizutani, W. Fabrication of Steady Junctions Consisting of *α*,*ω*-Bis(thioacetate) Oligo(*p*-phenylene vinylene)s in Nanogap Electrodes. *J. Am. Chem. Soc.* **2006**, *128*, 13720−13726.

(72) Tajima, K.; Li, L. S.; Stupp, S. I. Nanostructured Oligo(*p*-phenylene Vinylene)/Silicate Hybrid Films: One-Step Fabrication and Energy Transfer Studies. *J. Am. Chem. Soc.* **2006**, *128*, 5488−5495.

(73) Bredas, J. L.; Beljonne, D.; Coropceanu, V.; Cornil, J. Charge-Transfer and Energy-Transfer Processes in *π*-Conjugated Oligomers and Polymers: A Molecular Picture. *Chem. Rev.* **2004**, *104*, 4971−5004.

(74) Sasaki, S.; Niko, Y.; Klymchenko, A. S.; Konishi, G.-i. Design of Donor-Acceptor Geometry for Tuning Excited-State Polarization: Fluorescence Solvatochromism of Push-Pull Biphenyls with Various Torsional Restrictions on Their Aryl-Aryl Bonds. *Tetrahedron* **2014**, *70*, 7551−7559.

(75) Zöphel, L.; Enkelmann, V.; Müllen, K. Tuning the HOMO-LUMO Gap of Pyrene Effectively via Donor-Acceptor Substitution: Positions 4,5 Versus 9,10. *Org. Lett.* **2013**, *15*, 804−807.

(76) Yao, K.; Chen, L.; Chen, Y.; Li, F.; Ren, X.; Wang, H.; Li, Y. Tuning the Photovoltaic Parameters of Thiophene-Linked Donor-Acceptor Liquid Crystalline Copolymers for Organic Photovoltaics. *Polym. Chem.* **2012**, *3*, 710−717.

(77) Heredia, D.; Fernandez, L.; Otero, L.; Ichikawa, M.; Lin, C.-Y.; Liao, Y.-L.; Wang, S.-A.; Wong, K.-T.; Fungo, F. Electrochemical Tuning of Morphological and Optoelectronic Characteristics of Donor-Acceptor Spiro-Fluorene Polymer Film. Application in the Building of an Electroluminescent Device. *J. Phys. Chem. C* **2011**, *115*, 21907−21914.

(78) Zhang, H.; Wan, X.; Xue, X.; Li, Y.; Yu, A.; Chen, Y. Selective Tuning of the HOMO−LUMO Gap of Carbazole-Based Donor−Acceptor−Donor Compounds toward Different Emission Colors. *Eur. J. Org. Chem.* **2010**, *2010*, 1681−1687.

(79) Vijayakumar, C.; Tobin, G.; Schmitt, W.; Kim, M.-J.; Takeuchi, M. Detection of Explosive Vapors with a Charge Transfer Molecule: Self-Assembly Assisted Morphology Tuning and Enhancement in Sensing Efficiency. *Chem. Commun.* **2010**, *46*, 874−876.

(80) Liu, Y.; Zhon, J.; Wan, X.; Chen, Y. Synthesis and Properties of Acceptor-Donor-Acceptor Molecules Based on Oligothiophenes with Tunable and Low Band Gap. *Tetrahedron* **2009**, *65*, 5209−5215.

(81) Ajayaghosh, A.; Vijayakumar, C.; Praveen, V. K.; Babu, S. S.; Varghese, R. Self-Location of Acceptors as ″Isolated″ or ″Stacked″ Energy Traps in a Supramolecular Donor Self-Assembly: A Strategy to Wavelength Tunable FRET Emission. *J. Am. Chem. Soc.* **2006**, *128*, 7174−7175.

(82) Marsden, J. A.; Miller, J. J.; Shircliff, L. D.; Haley, M. M. Structure-Property Relationships of Donor/Acceptor-Functionalized Tetrakis(phenylethynyl)benzenes and Bis(dehydrobenzoannuleno)benzenes. *J. Am. Chem. Soc.* **2005**, *127*, 2464−2476.

(83) Wilson, J. N.; Bunz, U H. F. Switching of Intramolecular Charge Transfer in Cruciforms: Metal Ion Sensing. *J. Am. Chem. Soc.* **2005**, *127*, 4124−4125.

(84) Tour, J. M. Molecular Electronics. Synthesis and Testing of Components. *Acc. Chem. Res.* **2000**, *33*, 791−804.

(85) Bunz, U. H. F. Poly(aryleneethynylene)s: Syntheses, Properties, Structures, and Applications. *Chem. Rev.* **2000**, *100*, 1605−1644.

(86) Yamaguchi, Y.; Ochi, T.; Wakamiya, T.; Matsubara, Y.; Yoshida, Z. New Fluorophores with Rod-Shaped Polycyano *π*-Conjugated Structures: Synthesis and Photophysical Properties. *Org. Lett.* **2006**, *8*, 717−720.

(87) Yamaguchi, Y.; Tanaka, T.; Kobayashi, S.; Wakamiya, T.; Matsubara, Y.; Yoshida, Z. Light-Emitting Efficiency Tuning of Rod-Shaped *π* Conjugated Systems by Donor and Acceptor Groups. *J. Am. Chem. Soc.* **2005**, *127*, 9332−9333.

(88) Yamaguchi, Y.; Shimoi, Y.; Ochi, T.; Wakamiya, T.; Matsubara, Y.; Yoshida, Z. Photophysical Properties of Oligophenylene Ethynylenes Modified by Donor and/or Acceptor Groups. *J. Phys. Chem. A* **2008**, *112*, 5074−5084.

(89) Sonogashira, K. *Metal-Catalyzed Cross-Coupling Reactions*; Diederich, F., Stang, P. J., Eds.; Wiley-VCH: Weinheim, 1998.

(90) Sonogashira, K. *Comprehensive Organic Synthesis*; Trost, B. M., Fleming, I., Eds.; Pergamon: Oxford, U.K., 1991.

(91) Leventis, N.; Rawashdeh, A. -M. M.; Elder, I. A.; Yang, J.; Dass, A.; Sotiriou-Leventis, C. Synthesis and Characterization of Ru(II) Tris(1,10-phenanthroline)-Electron Acceptor Dyads Incorporating the 4-Benzoyl-N-methylpyridinium Cation or *N*-Benzyl-*N*′-methyl Viologen. Improving the Dynamic Range, Sensitivity, and Response Time of Sol-Gel-Based Optical Oxygen Sensors. *Chem. Mater.* **2004**, *16*, 1493−1506.

(92) Barltrop, J. A.; Coyle, J. D. *Principles of Photochemistry*; Wiley: New York, 1978; pp 68.

(93) Kober, E. M.; Caspar, J. V.; Lumpkin, R. R.; Meyer, T. J. Application of the Energy gap law to Excited-State Decay of Osmium(II)-Polypyridine Complexes: Calculation of Relative Non-radiative Decay Rates from Emission Spectral Profiles. *J. Phys. Chem.* **1986**, *90*, 3722−3734.

DOI: 10.1021/acs.jpca.5b05077
J. Phys. Chem. A XXXX, XXX, XXX−XXX

(94) Lin, S. H. *Radiationless Transitions*; Academic Press: New York, 1980.

(95) Griesser, H. S.; Wild, U. P. The Energy Gap Dependence of the Radiationless Transition Rates in Azulene and Its Derivatives. *Chem. Phys.* **1980**, *52*, 117−132.

(96) Gillipsie, G. D.; Lim, E. C. An Energy-Gap Correlation of Internal Conversion Rates. *Chem. Phys. Lett.* **1979**, *63*, 193−198.

(97) Frisch, M. J.; Trucks, G. W.; Schlegel, H. B.; Scuseria, G. E.; Robb, M. A.; Cheeseman, J. R.; Montgomery, J. A., Jr.; Vreven, T.; Kudin, K. N.; Burant, J. C.; et al. *Gaussian 03*, Revision C.02; Gaussian, Inc.: Wallingford, CT, 2004.

(98) Valeur, B. *Molecular Fluorescence*; Wiley-VCH: Weinheim, 2005.

(99) Yamaguchi, Y.; Matsubara, Y.; Ochi, T.; Wakamiya, T.; Yoshida, Z. How the π Conjugation Length Affects the Fluorescence Emission Efficiency. *J. Am. Chem. Soc.* **2008**, *130*, 13867−13869.

(100) Mataga, N.; Kaifu, Y.; Koizumi, M. Solvent Effects upon Fluorescence Spectra and the Dipole Moments of Excited Molecules. *Bull. Chem. Soc. Jpn.* **1956**, *29*, 465−470.

(101) Mataga, N.; Kaifu, Y.; Koizumi, M. The Solvent Effect on Fluorescence Spectrum. Change of Solute-Solvent Interaction During the Lifetime of Excited Solute Molecule. *Bull. Chem. Soc. Jpn.* **1955**, *28*, 690−691.

(102) Lippert, E. Dipole Moment and Electronic Structure of Excited Molecules. *Z. Naturforsch.* **1955**, *10a*, 541−545.

DOI: 10.1021/acs.jpca.5b05077
J. Phys. Chem. A XXXX, XXX, XXX−XXX